Performance of PtSn catalysts supported on MAl$_2$O$_4$ (M: Mg or Zn) in n-butane dehydrogenation: characterization of the metallic phase

Sonia A. Bocanegra[a], A. Guerrero-Ruiz[b], Sergio R. de Miguel[a], Osvaldo A. Scelza[a,*]

[a]Instituto de Investigaciones en Catálisis y Petroquímica, CenMat, Facultad de Ingeniería Química, Universidad Nacional del Litoral-CONICET, Santiago del Estero 2654, 3000 Santa Fe, Argentina
[b]Facultad de Ciencias, Universidad Nacional de Educación a Distancia, Madrid, Spain

Abstract

The Sn(0.3 or 0.5 wt.%) addition to Pt(0.3 wt.%)/ZnAl$_2$O$_4$ and Pt(0.3 wt.%)/MgAl$_2$O$_4$ catalysts leads to an increase of the activity and selectivity to olefins in the n-butane dehydrogenation reaction. Slight differences in the catalytic behaviour were found between 0.3 and 0.5 wt.% of Sn added to Pt in both catalyst series. Besides, the bimetallic catalysts also show a good stability through the five successive reaction-regeneration cycles, mainly the PtSn/MgAl$_2$O$_4$ one. The mono- and bimetallic catalysts were characterized by using different techniques: tests reactions of the metallic phase (cyclohexane dehydrogenation and cyclopentane hydrogenolysis), temperature programmed reduction, X-ray photoelectron spectroscopy, H$_2$ chemisorption, microcalorimetric measurements of the propylene adsorption and XRD. Results show that the nature of the metallic phase in monometallic samples appears to be different for the two supports. Thus, metallic particles with a very low concentration of hydrogenolytic sites (steps, corners and edges) would exist in the Pt/ZnAl$_2$O$_4$ catalyst in contrast with the structure of the metallic phase of the Pt/MgAl$_2$O$_4$ one, where the existence of an important concentration of hydrogenolytic sites is clearly observed (according to the cyclopentane hydrogenolysis results). The modification of Pt by the Sn addition clearly improves the catalytic behaviour in n-butane dehydrogenation due to important changes in the structure of the metallic phase. Thus, when Sn is added to Pt/ZnAl$_2$O$_4$ and Pt/MgAl$_2$O$_4$ catalysts the metallic surface structure seems to be more complex. In fact, results would indicate not only a partial formation of PtSn alloys or intermetallic compounds between Pt^0 and a fraction of Sn(0), but also a surface enrichment in Sn, dilution effects as well as the presence of tin stabilized on the support, probably as Sn(II/IV) oxides and SnCl$_2$ species.

1. Introduction

Bimetallic catalysts supported on ZnAl$_2$O$_4$ and MgAl$_2$O$_4$ have been found to be active and selective for the direct dehydrogenation of light paraffins. In fact, Padró et al. [1,2] found a very high selectivity to propylene (with values close to 97%) in the propane dehydrogenation for PtSn/ZnAl$_2$O$_4$ and PtGe/ZnAl$_2$O$_4$ catalysts. The PtSn/ZnAl$_2$O$_4$ catalysts used by Padró et al. [1] also showed a good catalytic

stability. At this respect, Rennard and Freel [3] found that the Pt/MgAl$_2$O$_4$ catalyst maintained a good Pt dispersion after several reaction-oxidation cycles (in propane and isopentane dehydrogenation reactions). Armendariz et al. [4] reported a good selectivity of PtSn/MgAl$_2$O$_4$ catalysts in the iso-pentane dehydrogenation to isoamilenes. Bosch et al. [5] and Aguilar-Ríos et al. [6] also showed a good performance of Pt and PtSn catalysts supported on ZnAl$_2$O$_4$ in isobutane dehydrogenation. Taking into account these behaviors, it would be also possible to use these supports in catalysts for dehydrogenation of linear paraffins with high molecular weight in order to produce the corresponding mono-olefins.

* Corresponding author. Tel.: +54 342 4555279; fax: +54 342 4531068.
E-mail address: oascelza@fiqus.unl.edu.ar (O.A. Scelza).

It must also be indicated that olefins have a very wide application in the production of polymers, intermediaries for detergents and additives for gasoline (MTBE) [7,8].

The use of $ZnAl_2O_4$ and $MgAl_2O_4$ as a support of PtSn is based on their neutral characteristics and very high thermal stability. The first characteristic is very important in paraffin dehydrogenation processes since a very high selectivity to olefins depends not only on adequate structure of the metallic phase but also on the low acidity of the support in order to minimize the undesirable lateral reactions (such as cracking and coke formation) [1,5].

One of the more relevant aspects in the study of these bimetallic systems is related to the knowledge of the structure of the metallic phase and its relationship with the catalytic behavior in the dehydrogenation of light paraffins, and with the methods used for the preparation of the support and the deposition of the metallic precursors. In fact, important aspects have not completely analyzed in the literature, viz, the probable alloy or intermetallic PtSn compounds formation [9], dilution effects of Pt by Sn, the interaction of the metallic phase with the support, the oxidation state of Sn, as well as the relationship between the catalytic stability and the modification of the structure of the metallic phase through successive reaction-regeneration cycles. Some investigations on the relationship between the surface structure and the catalytic behavior were reported in the literature for other bimetallic systems and reactions [10,11]. In consequence, the objective of this paper is to determine the effect of the Sn addition (0.3 and 0.5 wt.%) to Pt(0.3 wt.%) supported on $ZnAl_2O_4$ and $MgAl_2O_4$ over the catalytic performance (activity, selectivity, catalyst deactivation and stability) in the *n*-butane dehydrogenation reaction, which was carried out in flow and pulse equipments. It should be indicated that low Sn loadings were selected for this study since, according to the literature, the addition of higher amounts of Sn(1 wt.%) to Pt(0.5 wt.%)/$ZnAl_2O_4$ would produce the inhibition of the dehydrogenation activity [5]. Besides, a comparative study of the structure of the metallic phase of PtSn/$ZnAl_2O_4$ and PtSn/$MgAl_2O_4$ catalysts with low metal loadings (Pt: 0.3 wt.% and Sn: 0.3–0.5 wt.%) was performed. For this purpose, several characterization techniques were used: test reactions of the metallic phase (cyclohexane dehydrogenation and cyclopentane hydrogenolysis), temperature programmed reduction, X-ray photoelectron spectroscopy, H_2 chemisorption, microcalorimetric measurements of the propylene adsorption and X-ray diffraction.

2. Experimental

Two supports were used for the preparation of catalysts: $ZnAl_2O_4$ and $MgAl_2O_4$, which were synthesized following the technique reported by Strohmeier and Hercules [12]. In both cases, pure γ-Al_2O_3 was mixed with a stoichiometric amount of ZnO (from AnalaR, 99.9%) or MgO (from Alfa,

99.995%). These mixtures were ground to a very fine powder and then a small amount of deionized water was added in order to obtain a paste, which was first dried at 373 K for 6 h, and then subjected to a thermal treatment in an electric furnace at 1173 K for 72 h. Finally, the solid was ground to 35–80 mesh. In order to eliminate the excess of ZnO (or MgO), samples were submitted to an extraction treatment at room temperature with five portions of an aqueous solution of $(NH_4)_2CO_3$ (1 M). After the extraction procedure, the solid was separated from the liquid and dried at 383 K. The purified solid samples were X-ray diffracted (XRD) to confirm the elimination of the excess of ZnO or MgO species.

The textural properties of $ZnAl_2O_4$ and $MgAl_2O_4$ were determined in a Quantachrome Corporation NOVA 1000 surface area analyser, the S_{BET} values being 9.2 m^2 g^{-1} for $ZnAl_2O_4$ and 37 m^2 g^{-1} for $MgAl_2O_4$.

Monometallic Pt(0.3 wt.%) catalysts were prepared by impregnation of the corresponding support with an aqueous solution of H_2PtCl_6. For the impregnation of $ZnAl_2O_4$ and $MgAl_2O_4$, the Pt concentrations in the impregnating solutions were 4.3 and 2.15 g l^{-1}, respectively, and the impregnating volume/support weight ratios were 0.7 and 1.4 ml g^{-1}, respectively. In both cases the impregnations were carried out at room temperature for 6 h. Sn(0.5 wt.%) monometallic catalysts were prepared by impregnation of the corresponding support with a hydrochloric solution of $SnCl_2$ using the above mentioned impregnation volume/ support weight ratios. The Sn concentrations in the impregnating solutions were such as to obtain the desired Sn loading. After the impregnation, all the samples were dried at 383 K for 12 h.

The bimetallic catalysts: Pt(0.3 wt.%)Sn(0.3 wt.%)/ $ZnAl_2O_4$, Pt(0.3 wt.%)Sn(0.5 wt.%)/$ZnAl_2O_4$, Pt(0.3 wt.%)-Sn(0.3 wt.%)/$MgAl_2O_4$ and Pt(0.3 wt.%)Sn(0.5 wt.%)/ $MgAl_2O_4$ were obtained by impregnating the monometallic ones with a hydrochloric solution (1.2 M HCl) of $SnCl_2$. The Sn concentrations in the solutions were 4.28 and 7.14 g l^{-1} for the impregnation of Pt/$ZnAl_2O_4$ with 0.3 and 0.5 wt.% Sn, respectively. In the case of the impregnation of the Pt/$MgAl_2O_4$ with Sn, the concentrations were 2.14 g Sn l^{-1} for 0.3 wt.% Sn and 3.57 g Sn l^{-1} for 0.5 wt.% Sn. The ratio between the volume of the $SnCl_2$ solution and the weight of monometallic catalyst was 0.7 ml g^{-1} for Pt/$ZnAl_2O_4$ and 1.4 ml g^{-1} for Pt/ $MgAl_2O_4$. After the impregnation with the tin solution (6 h, 298 K), samples were dried at 383 K overnight. Then, mono- and bimetallic catalysts were calcined at 773 K for 3 h. These samples were labeled as fresh catalysts.

Two different *n*-butane dehydrogenation tests were carried out, one of them in a continuous flow reactor and the other one in a pulse equipment. The continuous flow experiments were performed at 803 K during 2 h in a quartz flow reactor heated by an electric furnace. The reactor (with a catalyst weight of 0.200 g) was fed with 18 ml min^{-1} of the reactive mixture (*n*-butane + hydrogen, H_2/*n*-C_4H_{10}

molar ratio = 1.25). The reactive mixture was prepared "in situ" by using mass flow controllers. All gases, n-butane, N_2 (used for purge), and H_2 (used for the previous reduction of catalysts and for the reaction) were high purity ones (>99.99%). Prior to the reaction, catalysts were reduced "in situ" at 803 K under flowing H_2 for 3 h. The reactor effluent was analysed in a GC-FID equipment with a packed chromatographic column (1/8 in. × 6 m, 20% BMEA on Chromosorb P-AW 60/80), which was kept at 323 K during the analysis. With this analytical device, the amounts of methane, ethane, ethylene, propane, propylene, n-butane, 1-butene, cis-2-butene, $trans$-2-butene and 1,3-butadiene were measured. The n-butane conversion was calculated as the sum of the percentages of the chromatographic areas of all the reaction products (except H_2) corrected by the corresponding response factor. The selectivity to the different reaction products (i) was defined as the ratio: mol of product i/ $\sum$ mol of all products (except H_2). Taking into account the high temperatures used for the reaction (for thermodynamic reasons), it was necessary to determine the contribution of the homogeneous reaction. For this purpose, a blank experiment was performed by using a quartz bed and the results showed a negligible n-butane conversion ($\ll 1\%$).

The pulse experiments were performed by injecting pulses of pure n-butane (0.5 ml STP) into the catalytic bed (0.100 g of sample) at 803 K. The catalytic bed was kept under flowing He (30 ml min^{-1}) between the injection of two successive pulses. Prior to the experiments, all samples were reduced "in situ" under flowing H_2 at 803 K for 3 h. The composition of each pulse after the reaction was determined by using a GC-FID equipment with a packed column (Porapack Q). The temperature of the chromatographic column was 303 K. In these experiments the n-butane conversion was calculated as the difference between the chromatographic area of n-butane fed to the reactor and the chromatographic area of non-reacted n-butane at the outlet of the reactor, and this difference was referred to the chromatographic area of n-butane fed to the reactor. The selectivity to a given product was calculated in the same way than for flow experiments. The carbon amount retained on the catalyst after the injection of each pulse was calculated through a mass balance between the total carbon amount fed to the reactor and the total carbon amount detected by the chromatographic analysis at outlet of the reactor. The accumulative carbon retention was calculated as the sum of the carbon amount retained after each pulse.

Besides the above mentioned test in n-butane dehydrogenation, studies on the catalytic stability of the bimetallic PtSn(0.3 wt.%)/ZnAl$_2$O$_4$ and PtSn(0.3 wt.%)/MgAl$_2$O$_4$ catalysts were carried out. These stability experiments consisted on five reaction-regeneration cycles. Each sequence was: reaction (at 803 K, 6 h), purge with N_2, regeneration with a O_2–N_2 mixture (5% (v/v) O_2) at 773 K for 6 h, purge with N_2 and reduction with H_2 at 803 K. The purge steps with N_2 were performed at 673 K for 30 min. The catalyst weight (0.500 g) used in these experiments was

higher than that of the flow experiments in order to magnify the thermal effects during the reaction, the regeneration (carbon burn-off, a very exothermic reaction) and the reduction (an exothermic reaction) steps.

The characteristics of the metallic catalysts were determined by different techniques: test reactions of the metallic phase (cyclohexane dehydrogenation and cyclopentane hydrogenolysis), temperature programmed reduction (TPR), X-ray photoelectron spectroscopy (XPS), H_2 chemisorption and microcalorimetric measurements of the propylene adsorption.

Cyclohexane dehydrogenation (CHD) and cyclopentane hydrogenolysis (CPH) were carried out in a differential flow reactor. Prior to these reactions, samples were reduced "in situ" with H_2 at the same temperature as the reaction was carried out. In both reactions the H_2/hydrocarbon molar ratio was 26. The reaction temperatures in CHD were 573 K for the catalysts supported on MgAl$_2$O$_4$ and 673 K for ZnAl$_2$O$_4$-based ones, whereas in CPH the temperature was 773 K for both catalyst series.

TPR experiments were performed in a quartz flow reactor. The samples (fresh and after five reaction-regeneration cycles) were heated at 6 K min^{-1} from room temperature up to about 900 K. The reductive mixture (5% (v/v) H_2–N_2) was fed to the reactor with a flow rate of 10 ml min^{-1}. Catalysts were previously calcined "in situ" at 773 K for 3 h.

XPS measurements were carried out in a VG-Microtech Multilab spectrometer, which operates with an energy power of 50 eV (radiation Mg Kα, $h\nu$ = 1253.6 eV). The pressure of the analysis chamber was kept at 4×10^{-10} Torr. Samples were previously reduced "in situ" at 803 K with H_2 for 2 h. Binding energies (BE) were referred to the C1s peak at 284.9 eV. The peak areas were estimated by fitting the experimental results with Lorentzian–Gaussian curves.

H_2 chemisorption measurements were made in a volumetric equipment. The sample was heated under flowing H_2 (60 ml min^{-1}) from room temperature up to 773 K, and then kept at this temperature for 4 h. Then, the sample was outgassed under vacuum (10^{-4} Torr) for 1 h. After the sample was cooled down to room temperature (298 K), the hydrogen dosage was performed in the range 50–250 Torr.

Microcalorimetric measurements of the propylene adsorption were carried out in a differential heat-flow microcalorimeter of the Tian-Calvet type (Setaram C80 II) operated under isothermal conditions. Samples contained into glass adsorption vessels were placed in the calorimeter. These vessels are linked to a volumetric apparatus that let the injection of successive small pulses of propylene. The equilibrium pressure was measured by means of a capacitance manometer (MKS Baratron 627). The temperature of the propylene adsorption was kept constant at 330 K. Catalysts were previously reduced "in situ" under flowing hydrogen at 773 K for 2 h, then outgassed at the same temperature for 16 h and finally cooled down to 330 K.

Table 1
Results of *n*-butane dehydrogenation in flow experiments

Catalyst	X^0, %	X^f, %	S^0, %	S^f, %	ΔX, %	Y^0, %	Y^f, %
Pt/ZnAl$_2$O$_4$	5.2	5.0	73.7	92.1	3.8	3.8	4.6
PtSn(0.3 wt.%)/ZnAl$_2$O$_4$	29.2	22.7	97.8	97.5	22.2	28.6	22.1
PtSn(0.5 wt.%)/ZnAl$_2$O$_4$	28.1	21.6	94.0	91.2	23.1	26.4	19.7
Pt/MgAl$_2$O$_4$	21.3	12.5	77.4	82.4	41.3	16.5	10.3
PtSn(0.3 wt.%)/MgAl$_2$O$_4$	32.1	27.0	97.8	98.9	15.9	31.4	26.7
PtSn(0.5 wt.%)/MgAl$_2$O$_4$	28.5	21.0	95.7	91.9	26.3	27.3	19.3

X^0: initial *n*-butane conversion and S^0: initial selectivity to all butenes (measured at 10 min of the reaction time). X^f: final *n*-butane conversion and S^f: final selectivity to all butenes (measured at 120 min of the reaction time). ΔX: $100(X^0 - X^f)/X^0$. Y^0 and Y^f: initial and final yields to all butenes (calculated as the product of the conversion and the selectivity to all butenes), respectively.

Afterwards, successive pulses of propylene were injected into the catalyst bed. The differential adsorption heats were obtained as the ratio between the exothermic heat value of each pulse and the adsorbed propylene amount. It is considered that the propylene monolayer is reached when the heat evolved falls in the physisorption field ($\leq$40 kJ mol^{-1}). The calorimetric and volumetric data were stored and processed with a microcomputer.

3. Results and discussion

3.1. Test in n-butane dehydrogenation

Table 1 shows the initial *n*-butane conversion (X^0, measured at 10 min of the reaction time) and final values of the *n*-butane conversion (X^f, measured at 120 min of the reaction time) both obtained from flow experiments for mono- and bimetallic catalysts supported on ZnAl$_2$O$_4$ and MgAl$_2$O$_4$. It can be observed that the Pt/ZnAl$_2$O$_4$ catalyst shows a very low *n*-butane conversion (about 5%) and this value is practically constant through the reaction, while the Pt/MgAl$_2$O$_4$ catalyst shows a higher initial conversion (21%). When Sn is added to the Pt/ZnAl$_2$O$_4$ catalyst the initial activities sharply increase reaching values close to 30% for both Sn contents. In a similar way, the Sn addition to the Pt/MgAl$_2$O$_4$ catalyst also increases the initial *n*-butane conversion.

Table 1 also shows the initial (S^0) and final (S^f) values of the selectivity to all butenes (1-butene, *cis*- and *trans*-2-butenes, and 1,3-butadiene) for mono- and bimetallic catalysts supported both on ZnAl$_2$O$_4$ and MgAl$_2$O$_4$. It can be observed that the initial selectivity of the Pt/ZnAl$_2$O$_4$ catalyst is about 73%, and then it increases reaching a value of 92% at the final reaction time. In the case of the Pt/MgAl$_2$O$_4$ catalyst, the initial selectivity is about 77% and then it slightly increases up to a final value of 82%. When Sn is added to the Pt/ZnAl$_2$O$_4$ catalyst, the initial selectivity to butenes is 94% for 0.5 wt.% of Sn and about 98% for 0.3 wt.% Sn. In the case of PtSn/MgAl$_2$O$_4$ catalysts, initial and final selectivity values to butenes range between 95 and 98%. The final selectivity values were similar for both catalyst series. It should be also noted that when the Sn loading increases from 0.3 up to 0.5 wt.%, the selectivities to

butenes are slightly modified for the bimetallic catalysts supported either on MgAl$_2$O$_4$ or ZnAl$_2$O$_4$.

Concerning to the deactivation parameter, ΔX, defined as $100 \times (X^0 - X^f)/X^0$ (where X^0 and X^f are the initial and final conversions, respectively), it can be observed a very low deactivation for the Pt/ZnAl$_2$O$_4$ catalyst. However, this sample shows a very low initial activity which is practically constant through the reaction. This behaviour could be due to the higher catalyst deactivation by coke deposition that could take place during the first minutes of the reaction. The effect of the initial deactivation by coke deposition can be better explained at the light of the pulse experiment results, as it will be analyzed below. On the other hand, the Pt/MgAl$_2$O$_4$ catalyst displays a very pronounced deactivation parameter (about 41%). When Sn is added to the Pt/MgAl$_2$O$_4$ catalyst, the deactivation parameter clearly decreases with respect to that of the monometallic one, mainly for 0.3 wt.% Sn. Table 1 also shows that PtSn(0.3 wt.%)/ZnAl$_2$O$_4$ and PtSn(0.5 wt.%)/ZnAl$_2$O$_4$ catalysts display similar deactivation parameter values. It can also be observed in Table 1 that the initial (Y^0) and final (Y^f) yields to all butenes (defined as the product between the *n*-butane conversion and the selectivity to all butenes) for the PtSn(0.3 wt.%) catalysts supported on both supports are slightly higher than the corresponding yields for catalysts with a higher Sn content (0.5 wt.%).

Eight pulses of pure *n*-butane were injected on each sample during the pulse experiments. Results of the *n*-butane conversion (X) as a function of the pulse number are indicated in Table 2. It can be observed that both monometallic catalysts display a high *n*-butane conversion after the injection of the first pulse. It is worth noticing that the initial activities of the monometallic catalysts in flow experiments are clearly lower than those of the bimetallic ones, mainly for the Pt/ZnAl$_2$O$_4$ catalyst, whereas the initial activities (first pulse) of the monometallic catalysts in pulse experiments are slightly higher than for the corresponding bimetallic ones (Table 2). The apparent increase of the initial activity for PtSn catalysts observed in flow experiments with respect to the monometallic ones can be explained by considering the results obtained in pulse experiments, mainly those of the relative carbon retention (RCR: defined as the accumulative carbon amount deposited after the injection of *i* pulses referred to the total carbon amount

Table 2
n-Butane conversion (*X*) and relative carbon retention (RCR) values as a function of the pulse number

Catalyst	Pulse number							
	1	2	3	4	5	6	7	8
Pt/ZnAl$_2$O$_4$								
X, %	64.4	61.8	55.7	52.2	50.8	48.3	40.9	38.0
RCR, %	19.5	36.8	50.8	62.8	74.6	85.5	93.3	100.0
PtSn(0.3 wt.%)/ZnAl$_2$O$_4$								
X, %	54.7	51.6	49.3	45.9	45.8	43.1	43.6	40.8
RCR, %	14.2	25.6	35.3	42.3	49.6	54.7	61.0	65.5
PtSn(0.5 wt.%)/ZnAl$_2$O$_4$								
X, %	53.9	51.8	50.5	49.4	48.4	47.9	47.0	46.0
RCR, %	13.2	24.1	33.7	42.4	50.4	58.0	65.2	70.9
Pt/MgAl$_2$O$_4$								
X, %	69.4	67.3	65.9	63.9	59.6	55.5	49.6	43.6
RCR, %	15.7	30.6	44.9	58.5	70.6	81.2	90.6	100.0
PtSn(0.3 wt.%)/MgAl$_2$O$_4$								
X, %	71.2	71.3	70.6	70.3	69.3	67.6	65.9	66.8
RCR, %	9.8	19.5	28.4	37.2	45.0	51.3	56.3	62.3
PtSn(0.5 wt.%)/MgAl$_2$O$_4$								
X, %	60.6	59.7	58.7	58.3	56.8	54.8	52.2	49.7
RCR, %	8.9	17.1	24.1	31.1	36.8	41.6	45.8	49.0

deposited on the corresponding monometallic catalyst after the injection of eight pulses). It can be observed in Table 2 that the relative carbon retentions after the injection of the first pulse for monometallic catalysts are not much different with respect to the bimetallic catalysts. However, the relative carbon retentions after the injection of eight pulses of *n*-butane for monometallic catalysts are clearly higher than for the corresponding bimetallic ones. It should be considered that the injection of the first pulse of *n*-butane is produced on a clean surface (carbon free), while the first *n*-butane conversion point obtained in the flow experiment (at 10 min

of the reaction time) corresponds to the reaction of *n*-butane on a partially deactivated surface by carbon deposition. Hence, taking into account the RCR values shown in Table 2, it is observed that the deactivation by coke deposition is more important for monometallic catalysts than for the bimetallic ones after the injection of the eight pulses of *n*-butane. In consequence, it can be expected a higher initial activity in bimetallic catalysts than for the monometallic ones at 10 min of the reaction time in flow experiments.

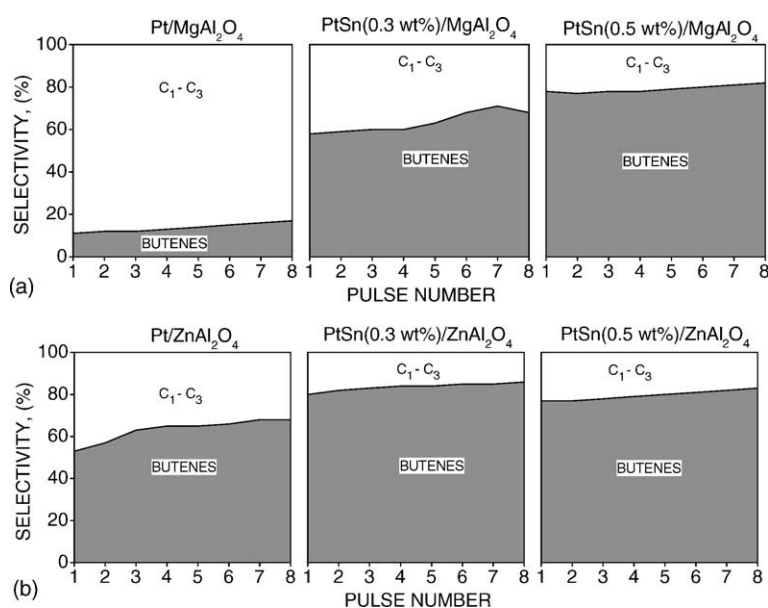With reference to the selectivity values in pulse experiments, Fig. 1a and b show that the selectivity slowly

Fig. 1. Selectivities to C$_1$–C$_3$ and to all butenes as a function of the pulse number for catalysts supported on (a) ZnAl$_2$O$_4$ and (b) MgAl$_2$O$_4$. Reaction temperature: 803 K.

increases as the pulse number increases. By comparing Fig. 1a and b, it can be observed that the hydrogenolytic capacity of Pt/MgAl$_2$O$_4$ is clearly higher than that of the Pt/ZnAl$_2$O$_4$ one. These behaviors are supported by the CPH reaction results, as it will be shown below. Besides, the Sn addition to Pt leads to an important increase of the selectivity to butenes (in pulse experiments), mainly for catalysts supported on MgAl$_2$O$_4$. It can be also observed that after the eighth pulse, the selectivity to butenes tends to reach a similar value for both Sn contents in the two catalysts series which agrees with the behaviour observed in flow experiments.

The results of the stability experiments are condensed in Figs. 2a, b and 3. Thus, Fig. 2a and b show the modification of the initial and final activities (n-butane conversion) and selectivities to all butenes for PtSn(0.3 wt.%)/MgAl$_2$O$_4$ and for PtSn(0.3 wt.%)/ZnAl$_2$O$_4$ catalysts, respectively, through the five successive reaction-regeneration cycles. It can be observed that the PtSn/MgAl$_2$O$_4$ catalyst shows a slight modification of the initial activity between the first and the fifth cycle. On the other hand, the decrease of the initial activity between the first and the fifth cycle for the PtSn/
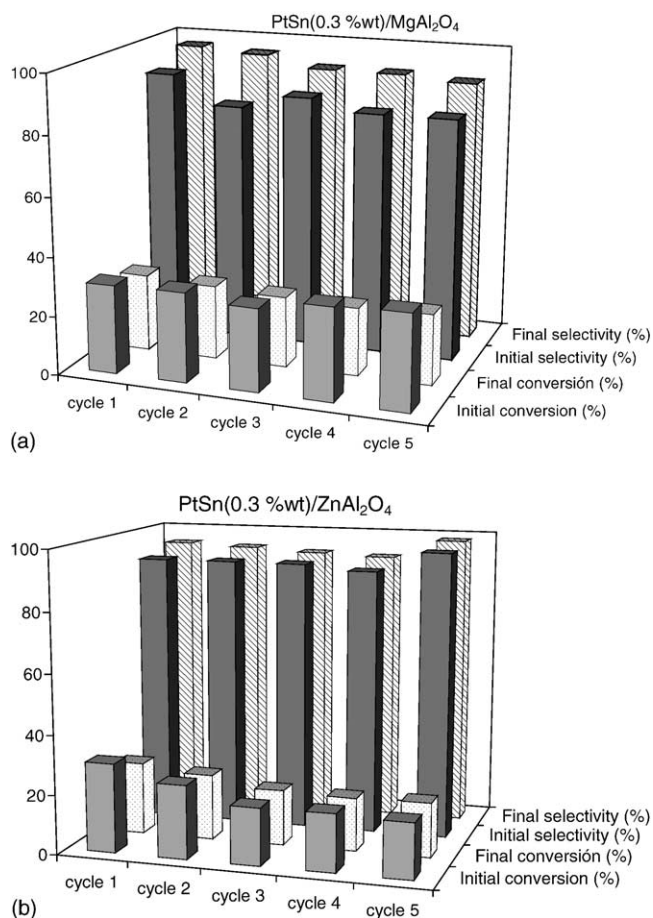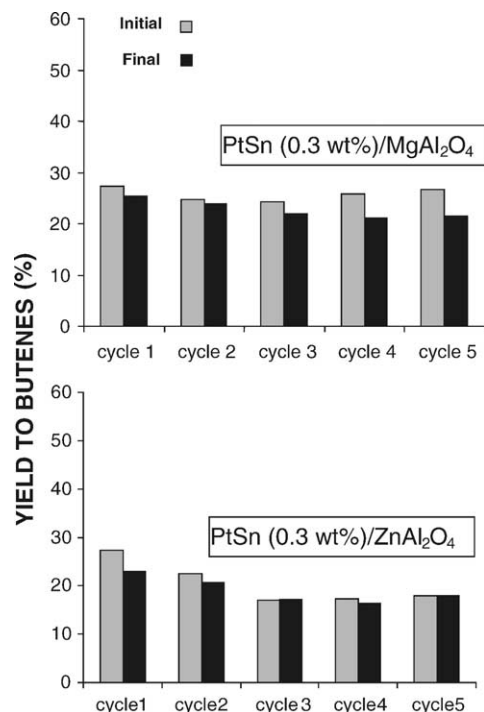

Fig. 3. Initial (at 10 min of the reaction time) and final (at 360 min of the reaction time) yields to butenes corresponding to PtSn(0.3 wt.%)/ZnAl$_2$O$_4$ and PtSn(0.3 wt.%)/MgAl$_2$O$_4$ catalysts for different cycles. Reaction temperature: 803 K.

ZnAl$_2$O$_4$ catalyst is clearly higher than for the PtSn/MgAl$_2$O$_4$ catalyst. In what the selectivity to all butenes it respects, it can be concluded that both PtSn/ZnAl$_2$O$_4$ and PtSn/MgAl$_2$O$_4$ catalysts display initial selectivity values (first cycle) of about 90% (Fig. 2a and b). Besides, the initial selectivity to all butenes displays a low modification through the successive cycles for the PtSn/ZnAl$_2$O$_4$ catalyst. In the case of the PtSn/MgAl$_2$O$_4$ catalyst, it can be observed a certain decrease of the initial selectivity to butenes through the successive cycles. In order to obtain a better comparison of the performance of both catalysts, the initial and final yields to all butenes for the different cycles were calculated as the product between the n-butane conversion and the selectivity to all butenes, and the results are shown in Fig. 3. The initial yield to butenes for the PtSn/MgAl$_2$O$_4$ catalyst is slightly modified through the successive cycles, and the final yield slowly decreases from 26% (first cycle) to 22% (fifth cycle). It can be also observed that the yield to butenes for the bimetallic catalyst supported on MgAl$_2$O$_4$ is clearly higher than for the bimetallic one supported on ZnAl$_2$O$_4$ through the successive cycles. In conclusion, these results indicate that the PtSn/MgAl$_2$O$_4$ catalyst is more stable than the PtSn/ZnAl$_2$O$_4$ one through the successive reaction-regeneration cycles.

3.2. Test reactions

Experiments of cyclohexane (CH) dehydrogenation were carried out on mono- and bimetallic catalysts supported on

Fig. 2. Initial n-butane conversion and selectivity to all butenes (at 10 min of the reaction time), and final n-butane conversion and selectivity to all butenes (at 360 min of the reaction time) for the different reaction-regeneration cycles (1–5) corresponding to (a) PtSn(0.3 wt.%)/ZnAl$_2$O$_4$ and (b) PtSn(0.3 wt.%)/MgAl$_2$O$_4$ catalysts. Reaction temperature: 803 K.

Table 3
Initial rates of cyclohexane dehydrogenation (R_{CH}) and cyclopentane hydrogenolysis (R_{CP}), activation energy for cyclohexane dehydrogenation (E_{CH}) and values of chemisorbed H_2 (H) for different catalysts

Catalyst	R_{CH} (mol/h g Pt)	E_{CH} (kcal/mol)	R_{CP} (mol/h g Pt, T = 773 K)	H (ml H_2 PTN/g cat)
Pt/ZnAl$_2$O$_4$	35.0[a]	16.8	Undetectable	0.023
PtSn(0.3 wt.%)/ZnAl$_2$O$_4$	5.3[a]	25.9	Undetectable	0.012
PtSn(0.5 wt.%)/ZnAl$_2$O$_4$	4.7[a]	27.6	Undetectable	0.016
Pt/MgAl$_2$O$_4$	52.1[b]	20.7	7.61	0.084
PtSn(0.3 wt.%)/MgAl$_2$O$_4$	20.8[b]	24.1	2.02	0.034
PtSn(0.5 wt.%)/MgAl$_2$O$_4$	0.2[b]	24.3	1.99	0.034

[a] Reaction temperature: 673 K.
[b] Reaction temperature: 573 K.

$MgAl_2O_4$ and $ZnAl_2O_4$ at 573 and 673 K, respectively, and the results are shown in Table 3. Catalysts supported on $ZnAl_2O_4$ were evaluated in this reaction at 673 K due to the negligible activity displayed at 573 K. The CH conversion for catalysts supported on $MgAl_2O_4$ at 673 K was very high ($\gg$10%) and under this condition the behaviour of the reactor is far from the differential flow reactor model, thus avoiding the correct measurement of the activation energy. Hence, the temperature selected for the CHD reaction on catalysts supported on $MgAl_2O_4$ was 573 K. Table 3 shows that there is an important decrease of the initial reaction rate and an increase of the activation energy for CHD reaction after the Sn addition to the Pt/ZnAl$_2$O$_4$ catalyst. In the case of catalysts supported on $MgAl_2O_4$, it can be observed that the monometallic one is very active at 573 K for CHD, and the addition of Sn to Pt sharply decreases the initial reaction rate, mainly for 0.5 wt.% Sn. The activation energies in CHD also increase after the Sn addition to the Pt/MgAl$_2$O$_4$ sample. The effect of the Sn addition to Pt on the activation energy appears to be more pronounced for bimetallic catalysts supported on $ZnAl_2O_4$ than for those supported on $MgAl_2O_4$. The increase of the activation energy in this structure-insensitive reaction [13] for both bimetallic catalysts with respect to the corresponding monometallic ones would indicate a modification of the active phase, probably due to interactions between both metals or alloy formation. By comparing the CHD results with those of the *n*-butane conversion in pulse experiments (first pulse, Table 2), it can be observed that the Sn addition to monometallic catalysts decreases the catalytic activity in both reactions (CH and *n*-butane dehydrogenations) though in a different magnitude.

Results of the cyclopentane hydrogenolysis (structure-sensitive reaction [14]) are also indicated in Table 3, which displays that the Pt/ZnAl$_2$O$_4$ catalyst has a negligible hydrogenolytic activity, in contrast to the important hydrogenolytic capacity of the Pt/MgAl$_2$O$_4$ one. These behaviors would be related to the influence of the support on the structure of the metallic particles. It should be noted that Aguilar-Ríos et al. [6,15], by using TEM measurements on Pt supported on $ZnAl_2O_4$ with high Pt loadings, observed no systematic orientation between the crystallographic planes of the support and those of the Pt particles, and these metallic particles would have a rounded shape with very low density

of steps and edges, which are the active sites for the hydrogenolysis reactions. On the other hand, the high hydrogenolytic activity of the Pt/MgAl$_2$O$_4$ catalyst at the same temperature (Table 3) indicates that the structure of the metallic phase of this catalyst would be different to that of the Pt/ZnAl$_2$O$_4$ one. It should be noted that the results obtained in pulse experiments also show that the Pt/MgAl$_2$O$_4$ catalyst display a much higher hydrogenolytic activity in *n*-butane dehydrogenation than the Pt/ZnAl$_2$O$_4$ one (Fig. 1a and b). According to Table 3, the CPH activity strongly decreases after the Sn addition to Pt/MgAl$_2$O$_4$, which indicates a very important diminution of the concentration of the metallic ensembles necessary for this reaction, probably due to a blocking or dilution effect of the Pt atoms by Sn. However, taking into account the CHD results, the formation of PtSn alloys cannot be discarded.

3.3. Temperature programmed reduction

Figs. 4 and 5 show the TPR profiles of fresh mono- and bimetallic catalysts supported on $MgAl_2O_4$ and $ZnAl_2O_4$, respectively. The TPR profiles of the PtSn(0.3 wt.%)/ZnAl$_2$O$_4$ and PtSn(0.3 wt.%)/MgAl$_2$O$_4$ bimetallic catalysts after five reaction-regeneration cycles are also included in these figures. The TPR profile of the fresh monometallic Pt/MgAl$_2$O$_4$ catalyst (Fig. 4) shows a main reduction peak at 538 K and a small peak at about 730 K. The presence of two reduction peaks was also observed in Pt/Al$_2$O$_3$ catalysts and it was explained by the existence of two different oxychlorinated Pt species originated after the impregnation of the support with chloroplatinic acid and the subsequent thermal treatments (drying and calcination steps) [16]. The TPR profile of the fresh Sn(0.5 wt.%)/MgAl$_2$O$_4$ catalyst shows a small, non-well-defined reduction zone at high temperatures ($>$650 K). Besides, the reduction profiles of the fresh bimetallic catalysts supported on $MgAl_2O_4$ show a main reduction peak (similar to that observed in the Pt/MgAl$_2$O$_4$) and a small H_2 consumption zone at 650–850 K. The main peaks for the monometallic samples are smaller than for the corresponding bimetallic ones, which are shifted to higher temperatures: 573 K for PtSn(0.3 wt.%)/MgAl$_2$O$_4$ and 580 K for PtSn(0.5 wt.%)/MgAl$_2$O$_4$.

The TPR profile of the fresh Pt/ZnAl$_2$O$_4$ catalyst (Fig. 5) shows only one reduction peak at 564 K. This peak is shifted
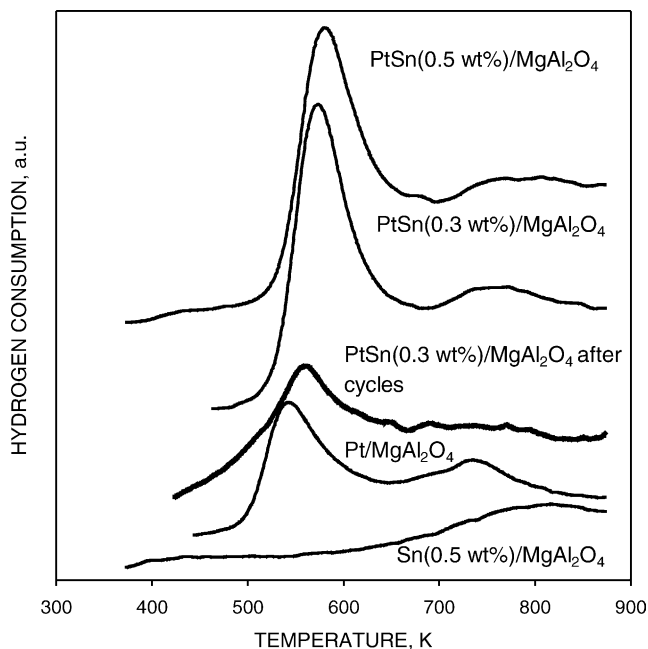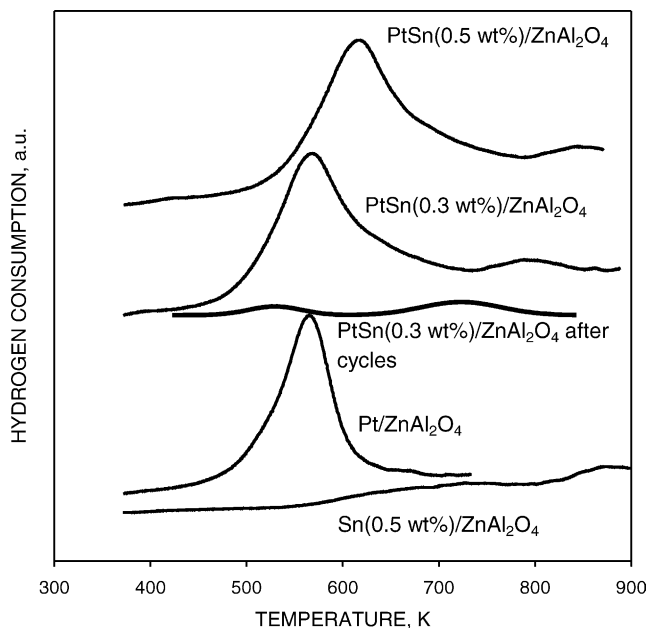
Fig. 4. TPR profiles of mono- and bimetallic (fresh and after five reaction-regeneration cycles) catalysts supported on $MgAl_2O_4$.

to higher temperatures in the bimetallic catalysts, appearing at 571 K for PtSn(0.3 wt.%)/$ZnAl_2O_4$ and at 616 K for PtSn(0.5 wt.%)/$ZnAl_2O_4$. It can be also observed that the TPR profiles of both fresh bimetallic catalysts show a small reduction zone at high temperatures, similar to that observed in the TPR profile of the Sn(0.5 wt.%)/$ZnAl_2O_4$ catalyst (Fig. 5).

By comparing the reduction profiles of the bimetallic catalysts with the corresponding profiles of monometallic Sn

Fig. 5. TPR profiles of mono- and bimetallic (fresh and after five reaction-regeneration cycles) catalysts supported on $ZnAl_2O_4$.

catalyst for each support series, it can be inferred that the reduction zone at high temperature in bimetallic catalysts could be attributed to the reduction of a small amount of Sn stabilized on the support. Moreover, the high area of the main peak observed in the bimetallic systems together with the shift to higher temperatures and the broadening of this peak after Sn addition to Pt could be related either to a catalytic effect of Pt on the Sn reduction (the hydrogen dissociated on Pt particles would reduce tin) or to a simultaneous reduction of both elements with probable alloy formation. Furthermore, Fig. 6 shows that the Sn addition to Pt produces an increase of the H_2 consumption in the TPR experiments, which can be related to a higher Sn reducibility in the bimetallic catalysts. It should be indicated that the H_2 consumption amounts for both monometallic Pt catalysts were such as to produce the total reduction of Pt to Pt^0.

It can be observed that the TPR profile of the PtSn/$ZnAl_2O_4$ catalyst after five reaction-regeneration cycles (Fig. 5) is very small, showing two reduction zones, one with a maximum at about 523 K and the other at 753 K. The shape of this TPR profile resembles the sum of the profiles of both monometallic catalysts, though with a very small first reduction peak, which is shifted to a lower temperature than the corresponding to the fresh Pt/$ZnAl_2O_4$ sample. The first peak can be assigned to the reduction of Pt species and the second one resembles the reduction of Sn species. According to Pakhomov et al. [17], an important fraction of metallic Pt is stabilized on the support after a calcination treatment of the PtSn/$ZnAl_2O_4$ catalyst. This can be the reason for the small first reduction peak (at low temperature) of the PtSn/$ZnAl_2O_4$ sample after the five reaction-regeneration cycles. In conclusion, an important fraction of metallic Pt would be stabilized on the support and the interaction between both metals appears to be decreased in the PtSn/$ZnAl_2O_4$ catalyst after the reaction-regeneration cycles. In the case of the TPR profile corresponding to PtSn/$MgAl_2O_4$ catalyst after the five reaction-regeneration cycles
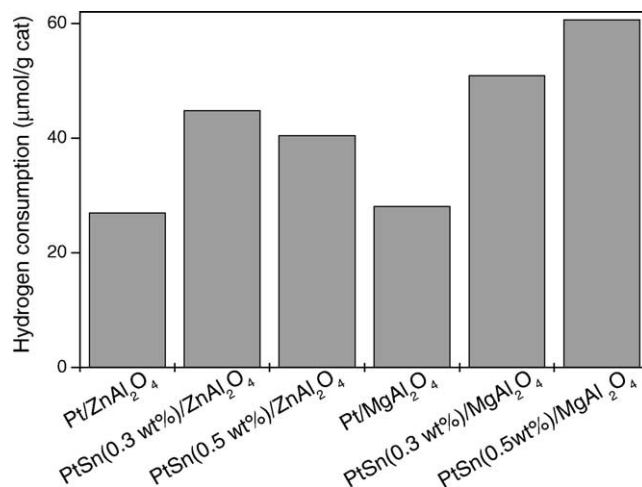

Fig. 6. H_2 consumption values in TPR experiments for different mono- and bimetallic catalysts.

(Fig. 4), it can be observed that the shape and the temperatures of the reduction peaks are very similar to that of the fresh sample, though these peaks have minor areas. This means that the metallic phase of this catalyst exhibits a higher stability than that supported on $ZnAl_2O_4$. These results would agree with the higher catalytic stability showed by the $PtSn/MgAl_2O_4$ sample through the reaction-regeneration cycles.

The modification of the structure of the metallic phase would take place from cycle to cycle. It should be taken into account that each cycle involves the reaction step, the burning of the deposited coke (exothermic reaction) and the reduction of the metal (exothermic process). All these effects can be involved in the modification of the metallic phase, though in a different degree according to the nature of the support.

3.4. X-ray photoelectron spectroscopy (XPS)

XPS spectra of the Pt 4f level for the $PtSn(0.5 \text{ wt.\%})/ZnAl_2O_4$ and $PtSn(0.5 \text{ wt.\%})/MgAl_2O_4$ catalysts reduced "in situ" at 803 K showed the doublets corresponding to zerovalent Pt 4f separated at 3.36 eV between them [18]. The doublets appear at 71.9 and 75.3 eV for the first catalyst and at 71.6 and 74.9 eV for the second one.

Fig. 7 shows the XPS spectra corresponding to the Sn $3d_{5/2}$ level of $Sn(0.5 \text{ wt.\%})/MgAl_2O_4$ and $PtSn(0.5 \text{ wt.\%})/MgAl_2O_4$ catalysts after reduction "in situ" at 803 K. From the deconvolution of the spectrum of the $Sn(0.5 \text{ wt.\%})/MgAl_2O_4$ catalyst, two peaks were obtained at 486.4 and 487.8 eV, corresponding to different types of oxidized Sn.
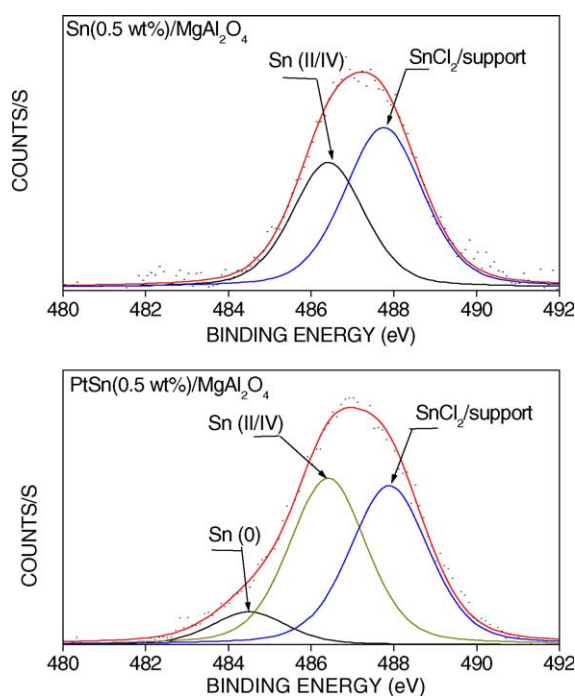
According to the literature, the line corresponding to Sn $3d_{5/2}$ for SnO has a BE at 486.5–486.8 eV, while the Sn $3d_{5/2}$ line for SnO_2 has a BE at 486.5 eV [18], therefore, it is not possible to discriminate the oxidation state of Sn corresponding to the signal positioned at 486.4 eV. In consequence, the first peak will be assigned to Sn(II)/Sn(IV) oxides, while the one at 487.8 eV could be probably due to chlorinated tin species bounded to the support according to the evidences reported in the literature [18,19]. From the deconvolution of the Sn $3d_{5/2}$ line of the spectrum corresponding to the $PtSn(0.5 \text{ wt.\%})/MgAl_2O_4$ catalyst, three peaks were also obtained at 484.5, 486.4 and 487.9 eV. The first one only appears in the XPS spectrum of the bimetallic catalyst and it would correspond to zerovalent Sn [18]. The second and the third peaks would be due to Sn(II)/Sn(IV) oxides and to chlorinated tin species bounded to the support, respectively, in a similar way as for the $Sn(0.5 \text{ wt.\%})/MgAl_2O_4$ sample.

Fig. 8 shows the XPS spectra corresponding to the Sn $3d_{5/2}$ level of $Sn(0.5 \text{ wt.\%})/ZnAl_2O_4$ and $PtSn(0.5 \text{ wt.\%})/ZnAl_2O_4$ catalysts after reduction "in situ" at 803 K. From the deconvolution of the spectrum of the $Sn(0.5 \text{ wt.\%})/ZnAl_2O_4$ catalyst, two peaks at 485.6 eV (Sn(II/IV) oxides) and at 487.5 eV ($SnCl_2$/support) were obtained. The spectrum of the Sn $3d_{5/2}$ level for the $PtSn/ZnAl_2O_4$ catalyst is similar to that of the $PtSn/MgAl_2O_4$ one and also shows three peaks at 484.5 eV (Sn(0)), 486.4 eV (Sn(II)/Sn(IV) oxides) and 487.9 eV ($SnCl_2$/support).

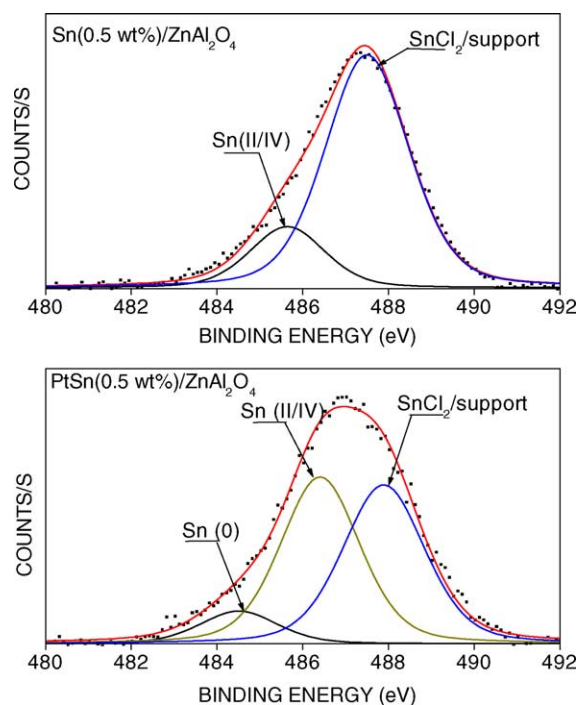The presence of Sn(0) in bimetallic catalysts and the absence of this species in the Sn monometallic one, would

Fig. 7. XPS spectra corresponding to the Sn $3d_{5/2}$ level for $Sn/MgAl_2O_4$ and $PtSn(0.5 \text{ wt.\%})/MgAl_2O_4$ catalysts, previously reduced at 803 K.

Fig. 8. XPS spectra corresponding to the Sn $3d_{5/2}$ level for $Sn/ZnAl_2O_4$ and $PtSn(0.5 \text{ wt.\%})/ZnAl_2O_4$ catalysts, previously reduced at 803 K.

indicate a higher Sn reducibility in PtSn catalysts, these results agreeing with the TPR ones.

Taking into account the above mentioned results for reduced bimetallic catalysts, it can be concluded that a fraction of Sn would be as Sn(0), probably alloyed with Pt, and the remaining Sn appears to be as Sn(II)/Sn(IV) oxides and chlorinated tin species bounded to the support. According to Figs. 7 and 8, the percentage of surface Sn(0) is similar for both bimetallic catalysts. Besides, from the XPS results surface atomic ratios of Sn/Pt was determined, which were 3.50 for PtSn(0.5 wt.%)/ZnAl$_2$O$_4$ and 4.38 for PtSn(0.5 wt.%)/MgAl$_2$O$_4$. Taking into account that both bimetallic catalysts have a bulk Sn/Pt atomic ratio of 2.74, it can be inferred that there is a certain surface enrichment in Sn in both catalysts, mainly for the PtSn(0.5 wt.%)/MgAl$_2$O$_4$ one.

3.5. Hydrogen chemisorption

Table 3 shows the values of the chemisorbed hydrogen volume on mono- and bimetallic catalysts supported on ZnAl$_2$O$_4$ and MgAl$_2$O$_4$. It can be observed that the chemisorption capacity of the Pt/ZnAl$_2$O$_4$ sample is clearly lower than that of the Pt/MgAl$_2$O$_4$ catalyst. This different behavior could be assigned to several causes: (1) the surface area of the ZnAl$_2$O$_4$ is lower than that of the MgAl$_2$O$_4$, (2) a different interaction of the metallic phase with these two supports and (3) a probable PtZn alloy formation in the Pt/ZnAl$_2$O$_4$ catalyst, mainly when the support is prepared from stoichiometric amounts of Al$_2$O$_3$ and ZnO, instead of using an excess of Al$_2$O$_3$ [6,20].

The value of the surface area of the support could lead to a different metal dispersion. However, the surface area should not be considered as the unique factor in this analysis, since the metal–support interaction could play an important role. Thus, Aguilar-Ríos et al. [6] have found by using energy dispersion spectroscopy (EDS) and HRTEM on Pt/ZnAl$_2$O$_4$ catalysts with low Pt contents, that a fraction of Pt would occupy the oxygen vacancies of the first layers of the spinel structure having a strong interaction with the support. This fraction of platinum appears as islands of electron deficient Pt species. Besides, these authors (by using XRD) did not detect metallic particles for low Pt loadings, probably due to the small size of these ones. However, these catalysts showed very low H$_2$ chemisorption capacities. These findings would indicate that the chemisorption value is not an adequate measurement of the Pt particle size for this type of catalyst. It must be remembered that Pakhomov and Buyanov [21] found that the PtCl$_6^{2-}$–ZnAl$_2$O$_4$ interaction was stronger than the PtCl$_6^{2-}$–MgAl$_2$O$_4$ one. Hence, it can be expected a lower possibility for the formation of electron deficient Pt islands in the first layer of the spinel structure of MgAl$_2$O$_4$ for the Pt/MgAl$_2$O$_4$ catalyst. In this sense, Table 3 shows a higher H$_2$ chemisorption capacity of the Pt/MgAl$_2$O$_4$ sample, this value being equivalent to Pt dispersion near to 50%.

With respect to the effect of the remaining impurities in the support after purification, it must be indicated that after the extraction treatment with (NH$_4$)$_2$CO$_3$ the XRD analysis did not show the characteristic ZnO lines in ZnAl$_2$O$_4$. However, an additional XRD experiment on Pt(1 wt.%)/ZnAl$_2$O$_4$ showed the characteristic lines of the Pt–Zn alloys (at d = 3.509, 2.219 and 1.747 Å) but with very low intensities. These lines are in agreement with the values reported in the literature for δ-PtZn alloy [20]. This alloy appears to be inactive for the hydrogen chemisorption, dehydrogenation of paraffins [20] and for the oxidation of isobutene [22]. However, this effect does not appear to be important for explaining the behavior of this monometallic catalyst in the H$_2$ chemisorption measurements. It should be also indicated that the formation of Pt–Mg alloys has not been reported in the literature [20].

The different behavior of Pt/ZnAl$_2$O$_4$ and Pt/MgAl$_2$O$_4$ catalysts in the H$_2$ chemisorption can be also related to the catalytic performance in n-butane dehydrogenation (flow experiments). In fact, the initial n-butane conversion for the Pt/MgAl$_2$O$_4$ sample is about four times higher than that for the Pt/ZnAl$_2$O$_4$ catalyst, and this value is very close to the H$_2$ chemisorption capacity ratio between these two catalysts.

When Sn is added to Pt (in both catalyst series) the chemisorption capacity decreases, mainly for the PtSn(0.5 wt.%)/MgAl$_2$O$_4$ sample. This behavior is parallel to the decrease of CHD reaction rate for both catalysts series. The decrease of the hydrogen adsorption capacity on both bimetallic catalysts is lower than the diminution of the CHD rate, probably due to different structural requirements between the H$_2$ chemisorption and the CHD reaction.
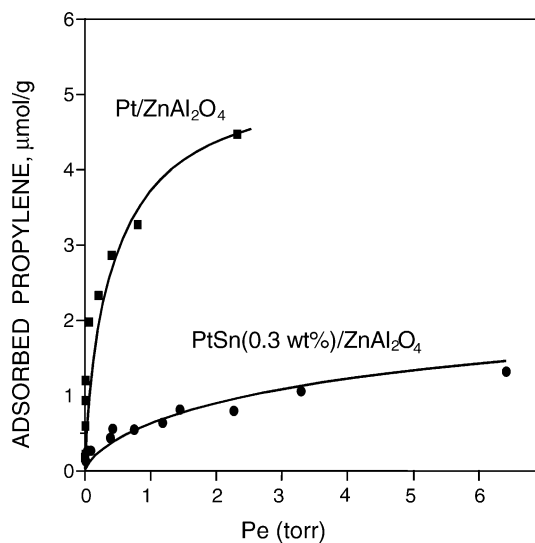

Fig. 9. Adsorption isotherms of propylene on Pt/ZnAl$_2$O$_4$ and PtSn(0.3 wt.%)/ZnAl$_2$O$_4$ catalysts at 330 K. Pe: equilibrium pressure of propylene.

3.6. Microcalorimetric measurements of propylene adsorption

Two different catalysts, $Pt/ZnAl_2O_4$ and $PtSn(0.3 wt.\%)/ZnAl_2O_4$, were evaluated by means of this technique. Fig. 9 shows the adsorption isotherms of propylene for both catalysts. It can be observed that the chemisorbed propylene amount for the monometallic catalyst is higher than for the bimetallic one. Fig. 10 shows the differential adsorption heats of propylene as a function of the propylene coverage (defined as the ratio between the amount of adsorbed propylene in a given point and that of the monolayer uptake). It can be observed that the propylene adsorption heats for the $Pt/ZnAl_2O_4$ catalyst are higher than for the $PtSn(0.3 wt.\%)/ZnAl_2O_4$ one in the overall range of the propylene coverage. Moreover, it can be appreciated in Fig. 10 that the Sn addition to $Pt/ZnAl_2O_4$ decreases the initial adsorption heat of the olefin (obtained by extrapolation of the curves to the propylene coverage equal to 0) from approximately $120 kJ mol^{-1}$ for the monometallic catalyst to approximately $80 kJ mol^{-1}$ for the bimetallic one. This lower initial adsorption heat of the olefin on the bimetallic catalyst would indicate that the binding energy between the alkene and the metallic site is weakened because of the Sn addition to Pt.

According to the literature [23], adsorption experiments of 1-hexene on Pt/Al_2O_3 and $PtSn/Al_2O_3$ catalysts indicate that the olefin is strongly adsorbed on Pt through the bonding of several carbon atoms placed in a flat position on the metallic surface. On the other hand, 1-hexene is weakly adsorbed on the bimetallic phase of PtSn, and the olefin would be placed in tilted or perpendicular position [23]. Moreover, several authors have studied the effect of the Sn addition to Pt supported on different materials on the
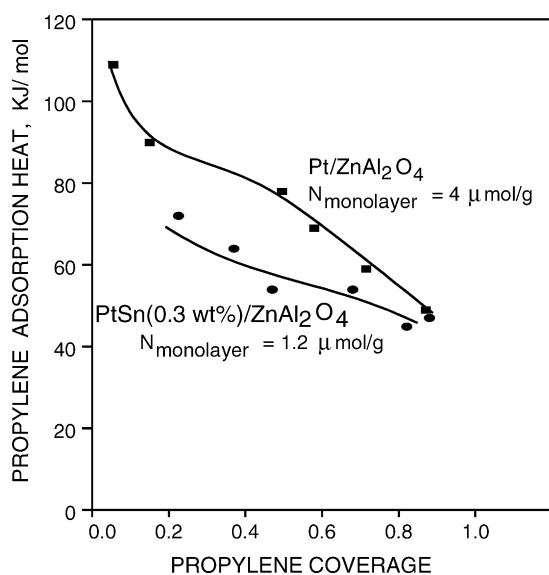

Fig. 10. Differential propylene adsorption heats at 330 K for $Pt/ZnAl_2O_4$ and $PtSn(0.3 wt.\%)/ZnAl_2O_4$ catalysts. $N_{monolayer}$: amount of propylene corresponding to the monolayer.

adsorption of ethylene and isobutene [24–26]. The combined results of microcalorimetric and spectroscopic studies suggest that the ethylene is dissociatively adsorbed on the platinum surface at room temperature producing ethylidyne species and adsorbed atomic hydrogen. On the contrary, the Sn addition to Pt suppresses the formation of these species, so that only the molecularly adsorbed ethylene is present at room temperature on the surface of Pt modified by Sn [25]. Besides, the higher initial adsorption heat of ethylene $(150 kJ mol^{-1})$ on the Pt surface at room temperature has been attributed to the dissociation of ethylene, while the lower initial adsorption heat $(115 kJ mol^{-1})$ on the bimetallic PtSn phase can be explained by the presence of ethylene molecules adsorbed on the surface [25]. It has been reported that the Sn addition to Pt/SiO_2 reduces the initial adsorption heat of isobutene from 185 to $125 kJ mol^{-1}$ [24]. The higher adsorption heat of isobutene on the monometallic catalyst was attributed to the dissociation of the olefin, whereas the lower isobutene adsorption heat on the bimetallic catalyst can be caused by the presence of isobutene adsorbed in a molecular way [24]. These authors concluded that the Sn addition to Pt reduces the actual size of surface Pt ensembles by geometric and/or electronic effects, and in consequence it suppresses the formation of highly dehydrogenated surface species.

Considering these bibliographic reports, our results of the microcalorimetric measurements of the propylene adsorption on $Pt/ZnAl_2O_4$ and $PtSn/ZnAl_2O_4$ catalysts could be interpreted taking into account that the high initial propylene adsorption heat on the $Pt/ZnAl_2O_4$ surface could be attributed to the dissociation of the olefin into propylidyne species and adsorbed atomic hydrogen, while the lower adsorption heat of propylene on the $PtSn/ZnAl_2O_4$ surface would be caused by the adsorption of molecular propylene. From these evidences it can be concluded that the presence of Sn in the vicinity of Pt would produce a decrease both in the size of the Pt ensembles and the Pt–olefin interaction strength, by geometric and electronic effects. Therefore, once the olefin is formed (from the paraffin dehydrogenation) it is immediately desorbed, avoiding the formation of the coke precursors by a further dehydrogenation reaction on the bimetallic catalyst. Hence, an increase of the dehydrogenation selectivity and a lower formation of carbonaceous deposits could be expected for the bimetallic catalysts, such as, it can be observed from pulse experiment results. On the other hand, the surface of the monometallic catalyst would be composed by large Pt ensembles, which would strongly adsorb the olefins in a dissociative way (when it is produced), followed by the dehydrogenation to coke precursors, thus increasing the carbon deposition.

4. Conclusions

From the evidences presented in the paper the following conclusions can be obtained:

1. The Sn addition to $Pt/ZnAl_2O_4$ and $Pt/MgAl_2O_4$ leads to an increase of the activity in *n*-butane dehydrogenation, and to high selectivity values to all butenes (1-butene, *cis*- and *trans*-2-butenes, and 1,3-butadiene). Besides, these bimetallic catalysts show low deactivation parameter values (close to 20%) and the yields to all butenes for the PtSn(0.3 wt.%) catalysts supported on both supports are slightly higher than for catalysts with a higher Sn content (0.5 wt.%).

2. PtSn catalysts supported on $ZnAl_2O_4$ and $MgAl_2O_4$ show good catalytic stability levels after five reaction-regeneration cycles, though the stability of the $PtSn/MgAl_2O_4$ catalyst was clearly higher than for the $PtSn/ZnAl_2O_4$ one. These behaviors can be related to the higher stability of the metallic phase for the first catalyst after the five successive reaction-regeneration cycles, according to the TPR results.

3. The structure of the metallic phase of the $Pt/ZnAl_2O_4$ catalyst appears to be different from that of the $Pt/MgAl_2O_4$ one. In the first case, the metallic particles have a very low hydrogenolytic capacity (according to CPH results). In the case of $Pt/MgAl_2O_4$, the metallic particles display an important concentration of hydrogenolytic centers. The different hydrogenolytic capacities between $Pt/ZnAl_2O_4$ and $Pt/MgAl_2O_4$ catalysts can explain the very different selectivities to butenes found in the pulse experiments.

4. When Sn is added to $Pt/MgAl_2O_4$ and $Pt/ZnAl_2O_4$ catalysts, the tin reducibility is increased by either the catalytic effect of platinum or the PtSn co-reduction with probable alloy formation. Besides, a very complex structure of the metallic phase appears to be present in the bimetallic catalysts. In fact, a probable description of this phase would involve the presence of Pt in zerovalent state, which could be partially alloyed with a fraction of zerovalent tin (according to CHD results). Taking into account the XPS results, these alloy particles coexist with other species: oxidized Sn, which could be stabilized on the support and segregated on the surface of the metallic phase, and $SnCl_2$ species supported on the aluminates. Oxidized Sn species could produce both the blocking of the zerovalent Pt atoms and the dilution of the active centers. These effects lead to a decrease of the concentration of Pt ensembles necessary for the hydrogenolysis reactions and the coke deposition (according to CPH, dehydrogenation of *n*-butane in pulse experiments and microcalorimetric results of propylene adsorption). Then, when these catalysts are used in paraffin dehydrogenation, the selectivity to olefins is increased because the formation of lower paraffins by hydrogenolysis is sharply decreased, and the carbon deposition is also diminished, thus improving the catalytic performance of the bimetallic catalysts.

References

[1] C.L. Padró, S.R. de Miguel, A.A. Castro, O.A. Scelza, Stud. Surf. Sci. Catal. 111 (1997) 191.
[2] C.L. Padró, S.R. de Miguel, A.A. Castro, G.T. Baronetti, O.A. Scelza, in: Proceedings of the XV Iberoamerican Symposium on Catalysis, vol. 1, Argentina, 1996, p. 507.
[3] R.J. Rennard, J. Freel, J. Catal. 98 (1986) 235.
[4] H. Armendariz, A. Guzmán, A. Toledo, M.A. Llanos, A. Vázquez, G. Aguilar, in: Proceedings of XVII Iberoamerican Symposium on Catalysis, Portugal, 2000, p. 105.
[5] P. Bosch, M.A. Valenzuela, B. Zapata, D. Acosta, G. Aguilar-Ríos, C. Maldonado, I. Shifter, J. Molec. Catal. 93 (1994) 67.
[6] G. Aguilar-Ríos, M.A. Valenzuela, H. Armendáriz, P. Salas, J.M. Domínguez, D.R. Acosta, I. Schifter, Appl. Catal. A: General 90 (1992) 25.
[7] L.F. Hatch, S. Matar, From Hydrocarbons to Petrochemicals, Gulf Publishing Company, Houston, 1981.
[8] A.V. Hahn, The Petrochemical Industry, Mc Graw-Hill Inc., New York, 1970.
[9] N.A. Pakhomov, R.A. Buyanov, E.M. Moroz, E.N. Yurchenko, A.P. Chernyshev, N.A. Zaitseva, G.R. Kotelnikov, React. Kinet. Catal. Lett. 14 (1980) 329.
[10] J.M. Ramallo-López, G.F. Santori, L. Giovanetti, M.L. Casella, O.A. Ferretti, F.G. Requejo, J. Phys. Chem. B 107 (2003) 11441.
[11] T.W. Hansen, J.B. Wagner, P.L. Hansen, S. Dahl, H. Topsøe, C.J.H. Jacobsen, Science 294 (2001) 1508.
[12] B.R. Strohmeier, D.M. Hercules, J. Catal. 86 (1984) 266.
[13] A.D. Cinneide, J.K.A. Clarke, Catal. Rev. 7 (1972) 233.
[14] M. Boudart, Adv. Catal. 20 (1969) 153.
[15] G. Aguilar-Ríos, M.A. Valenzuela, D.R. Acosta, I. Shifter, et al. in: L. Guczi (Ed.), Proceedings of the 10th International Congress on Catalysis, Hungary, 1992, p. 1831.
[16] G. Lietz, H. Lieske, H. Spindler, W. Hanke, J. Völter, J. Catal. 81 (1983) 17.
[17] N.A. Pakhomov, R.A. Buyanov, E.N. Yurchenko, A.P. Chernyshev, G.R. Kotelnikov, E.M. Moroz, A.A. Zaitseva, A. Patanov, Kinetika i Kataliz 22 (1981) 488.
[18] C.D. Wagner, W.M. Riggs, L.E. Davis, J.F. Moulder, Handbook of X-ray Photoelectron Spectroscopy, 1993.
[19] J.M. Stencel, J. Goodman, B.H. Davis, in: Proceedings of the 9th International Congress on Catalysis, Calgary, Canada, 1988, p. 1291.
[20] N.A. Pakhomov, R.A. Buyanov, E.M. Moroz, G.R. Kotelnikov, V.A. Patanov, React. Kinet. Catal. Lett. 9 (1978) 257.
[21] N.A. Pakhomov, R.A. Buyanov, Stud. Surf. Sci. Catal. 91 (1995) 1101.
[22] M. Zawadzki, W. Mista, L. Kepinski, Vacuum 63 (2001) 291.
[23] H. Lieske, A. Sárkány, J. Völter, Appl. Catal. 30 (1987) 69.
[24] R.D. Cortright, J.M. Hill, J.A. Dumesic, Catal. Today 55 (2000) 213.
[25] R.D. Cortright, J.A. Dumesic, J. Catal. 148 (1994) 771.
[26] F.B. Passos, M. Schmal, M.A. Vannice, J. Catal. 160 (1996) 118.